determined as much as kinetic as by equilibrium considerations. This is particularly critical for any proposed catalytic cycle. Clearly, several questions must be answered before the pronounced stereoselectivity reported here for the cis(N,olefin) isomers of mixed olefin–amino acid complexes containing chiral nitrogens can be employed to direct reliably the stereochemistry of reactions of coordinated prochiral olefins in the same molecule.

The relative ease with which 2-mb and allOH can be displaced by other olefins makes it readily possible to convert *cis*-Pt(sar)(2-mb)Cl and *cis*-Pt(*S*-pro)(2-mb)Cl to other cis(N,olefin) compounds in order to compare the degree of stereoselectivity for a series of prochiral olefins. The relative importance of the OH group, the length of the hydrocarbon chain, the degree of branching of the chain, and the effect of aromatic substituents can be determined by comparing the isomer ratios for such a series. Such efforts are currently being pursued in our laboratory to further clarify the role of specific structural features that are responsible for the extraordinary stereoselectivity which these compounds exhibit.

Acknowledgment is made to the donors of the Petroleum Research Fund, administered by the American Chemical Society, for support of this research, to the Pew Charitable Trust and the National Science Foundation for support for the NMR spectrometer used in this work, and to the Pew Mid-States Consortium for a Faculty Development Award (L.E.E.). The able assistance of Marufar Rahim (VT) and Peter Hayes (Grinnell) is gratefully acknowledged.

Supplementary Material Available: For the three structures reported, additional illustrations of NMR spectra (^1H, ^{13}C, ^{195}Pt) of some of the amino acid–olefin complexes and tables listing crystal data, anisotropic thermal parameters of the non-hydrogen atoms, and atomic coordinates and isotropic thermal parameters of the hydrogen atoms (7 pages); tables of observed and calculated structure factors (29 pages). Ordering information is given on any current masthead page.

Contribution from the URA 405 du CNRS, Electrochimie et Physico-Chimie des Complexes et des Systèmes Interfaciaux, and IBMC du CNRS, Laboratoire de Cristallographie Biologique, Institut de Chimie, Université Louis Pasteur, 1, rue Blaise Pascal, B.P. 296R8, 67008 Strasbourg Cedex, France

Trinuclear Copper(II) Hydroxo and Hexanuclear Copper(II) Oxo Complexes with the Ligand 3-(Benzylimino)butanone 2-Oxime. Syntheses and Spectral, Structural, and Redox Characteristics

Y. Agnus,* R. Louis, B. Metz, C. Boudon, J. P. Gisselbrecht, and M. Gross

Received December 28, 1990

The syntheses, structures, and properties of a trinuclear copper(II) hydroxo complex and a hexanuclear copper(II) oxo complex containing the same imino–oximato ligand are reported. The pair $[Cu_3(\mu_3\text{-}OH)L_3(ClO_4)_2(H_2O)]$ (**1**) and $[Cu_6(\mu_4\text{-}O)_2L_6(H_2O)](ClO_4)_2\cdot 0.5H_2O$ (**2**) displays the first example of tri- and hexacopper(II) complexes built with the same ligand, 3-(benzylimino)butanone 2-oxime (LH). The X-ray crystallographic structures have been determined. **1** crystallizes in the monoclinic space group $P2_1/c$ (a = 15.350 (1) Å, b = 12.508 (1) Å, c = 21.439 (2) Å, β = 96.81 (1)°, Z = 4). The molecular structure shows that the copper ions are at the corners of an equilateral triangle, separated by 3.25 Å, held together by a μ_3-hydroxo group and three oxime bridges. An unusual triply coordinated perchlorate ion interacts in axial position with the three copper ions. **2** crystallizes in the monoclinic space group $P2_1/n$ (a = 15.622 (2) Å, b = 27.025 (2) Å, c = 18.864 (4) Å, β = 97.38 (2)°, Z = 4). Here the $[Cu_6(\mu_4\text{-}O)_2L_6]^{2+}$ cation contains two triangular $[Cu_3O]$ units, bridged by their central oxygen atoms. The electron-transfer properties of **1** and **2** in propylene carbonate solution have been studied by voltammetry, coulometry, and spectrophotometry. **1** is electroreducible into a $[Cu^ICu^{II}_2(OH)]^+$ species at −0.41 V versus SCE, followed by a fast chemical step leading to another $[Cu^ICu^{II}_2(OH)]^+$ entity, **3**, which is reversibly oxidizable at +0.42 V versus SCE. **2** is reversibly electrooxidizable at +0.42 V versus SCE into a $[Cu^{III}Cu^{II}_2(O)]^{2+}$ species, **4**, which transforms slowly through an homogeneous reaction into **1**. Reversible and quantitative interconversion between **1** and **2** is achieved by protonation/deprotonation of the μ_3-oxygen. This proton gated reaction grants to the species either a mild oxidant (**1**) or a mild reductant (**2**) character. The similarity of the redox potential for the couples $[Cu^ICu^{II}_2(OH)]^+/[Cu^{II}Cu^{II}_2(OH)]^{2+}$ involving **3** and $[Cu^{II}_3(O)]^+/[Cu^{III}Cu^{II}_2(O)]^{2+}$ involving **2** makes **1** act as a chemical switch between two loops of redox reaction chains.

Introduction

Triangular copper(II) complexes have been extensively studied, especially regarding their magnetic, structural, and redox characteristics,[1-22] in relation to their interest in copper–proteins interactions and to homogeneous catalysis. μ-Hydroxo[1-20] or μ-oxo ions[6,15-22] have generally been observed as central bridging ligands. In the oxo derivatives, the oxygen atom is nearer the plane of the three copper ions (0.35 Å)[6] than in the hydroxo derivatives (0.48–0.93 Å).[4-6,8-10,12,13,16] These complexes exhibit identical, all different, or only two different copper stereochemistries. The coordination polyhedron of each metallic ion is a distorted octahedron. The three equatorial arrays are usually nearly coplanar, although orthogonal orientation with respect to the {3Cu} plane have been reported.[7-12]

Electrochemical studies have shown that monoelectronic transfers are possible: the $[Cu_3(\mu\text{-oxo})]$ groups are electrooxidizable,[18-21] generating $[Cu^{III}Cu^{II}_2]$ complexes, whereas the $[Cu_3(\mu\text{-hydroxo})]$ groups are electroreducible to $[Cu^ICu^{II}_2]$ compounds.[19,20]

* To whom correspondence should be addressed at Institut de Chimie, Université Louis Pasteur.

(1) Green, R. W.; Svasti, M. C. K. *Aust. J. Chem.* **1963**, *16*, 356–359.
(2) Beckett, R.; Colton, R.; Hoskins, B. F.; Martin, R. L.; Vince, D. G. *Aust. J. Chem.* **1969**, *22*, 2527–2533.
(3) Hoskins, B. F.; Vince, D. G. *Aust. J. Chem.* **1972**, *25*, 2039–2044.
(4) Beckett, R.; Hoskins, B. F. *J. Chem. Soc., Dalton Trans.* **1972**, 291–295.
(5) Hulsbergen, F. B.; ten Hoedt, R. W. M.; Verschoor, G. C.; Reedijk, J.; Spek, A. L. *J. Chem. Soc., Dalton Trans.* **1983**, 539–545.
(6) Butcher, R. J.; O'Connor, C. J.; Sinn, E. *Inorg. Chem.* **1981**, *20*, 537–545.
(7) Comarmond, J.; Dietrich, B.; Lehn, J. M.; Louis, R. *J. Chem. Soc., Chem. Commun.* **1985**, 74–76.
(8) Costes, J. P.; Dahan, F.; Laurent, J. P. *Inorg. Chem.* **1986**, *25*, 413–416.
(9) Kwiatkowski, M.; Kwiatkowski, E.; Olechnowicz, A.; Ho, D. M.; Deutsch, E. *Inorg. Chim. Acta* **1988**, *150*, 65–73.
(10) Ahlgren, M.; Turpeinen, U.; Smolander, K. *Acta Crystallogr., Sect. B* **1980**, *B36*, 1091–1095.
(11) Butcher, R. J.; Overman, J. W.; Sinn, E. *J. Am. Chem. Soc.* **1980**, *102*, 3276–3278.
(12) Smolander, K. *Acta Chem. Scand.* **1983**, *A37*, 5–13.
(13) Bailey, N. A.; Fenton, D. E.; Moody, R.; Scrimshire, P. J.; Beloritzky, E.; Fries, P. H.; Latour, J. M. *J. Chem. Soc., Dalton Trans.* **1988**, 2817–2824.

0020-1669/91/1330-3155$02.50/0

The magnetic exchange properties of these triangular Cu(II) species[23] result from large antiferromagnetic interactions, documented by a strong exchange coupling constant ranging up to 350 cm^{-1}. The low magnetic moment observed over a large temperature range is consistent with a single electron per trinuclear unit ($S = {}^1/_2$) in the ground state.[1-3,5,6,8,9,13,15,17,22] Until now, no EPR signals were observed at room temperature and only ill-resolved spectra were obtained at low temperatures.[5,8,9,13,21]

The association of two parallel triangular Cu_3 species leads to bis(hydroxo),[5,10-13] bis(oxo),[6] or oxo–hydroxo[15] hexacopper complexes. A similar "dimerization" of a square tetracopper(II) complex has been reported.[24,25] A tetranuclear bis(hydroxo) complex has been observed.[14]

This paper reports the syntheses, X-ray structures, spectral characteristics, and redox properties of tri- and hexacopper(II) imino–oximato complexes with the ligand 3-(benzylimino)butanone 2-oxime (LH). In the hydroxo complex $[Cu_3(\mu_3\text{-}OH)L_3(ClO_4)_2(H_2O)]$ (**1**), the $[Cu_3(\mu_3\text{-}OH)]$ core is capped by an unusual triply coordinated perchlorate ion. In basic media, **1** transforms into the hexacopper(II) bis(oxo) complex $[Cu_6(\mu_4\text{-}O)_2L_6(H_2O)](ClO_4)_2\cdot 0.5H_2O$ (**2**). The couple **1** and **2** is the first example involving *the same organic ligand* in distinct identified hydroxo and oxo forms. Thus an interesting opportunity is provided to rationalize their physical and chemical properties. The detailed understanding of their redox properties associated with the **1** ↔ **2** interconversion driven by protonation/deprotonation displays original relationships between the species.

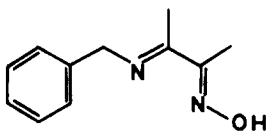

LH

Experimental Section

Techniques. UV–visible spectroscopic measurements were carried out on a Shimadzu UV260 spectrometer. IR spectra were obtained on KBr pellets with a Bruker FTIR25 spectrometer. ^1H NMR spectra were recorded on a Bruker S4 200 spectrometer. EPR measurements were made with a X-band Bruker ER100 spectrometer at Institut C. Sadron, CNRS, Strasbourg, France. Low-temperature spectra down to 77 K involved the use of a standard liquid-nitrogen cryostat. X-ray fluorescence experiments were made at Laboratoire de Chimie nucléaire, CRN-CNRS, Strasbourg, France. Elemental analyses were performed by the Service de Microanalyse de l'Institut de Chimie, Strasbourg, France. *Caution! Perchlorate derivatives may detonate upon scraping or heating.*

Synthesis of 3-(Benzylimino)butanone 2-Oxime (LH). LH was prepared by condensation of benzylamine with 2,3-butanedione oxime using an adapted procedure.[26] The reaction workup was simplified, and the yield was enhanced when the reactions were carried out under argon with freshly distilled benzylamine and isopropyl ether. Recrystallization from methanol–isopropyl ether gave white needles, which decomposed in air. Yield: 70%. $C_{11}H_{14}N_2O$: mp 98–100 °C. ^1H NMR ($CDCl_3$): δ 2.150 (s, 3 H, CH_3–C(imino)), 2.175 (s, 3 H, CH_3–C(oximato)), 4.697 (s, 2 H, $-CH_2$–N(imino)), 7.322–7.393 (m, 5 H, C–*H* aromatic).

Table I. Crystallographic Data for **1** and **2**

	complex **1**	complex **2**
formula	$C_{33}H_{42}Cl_2Cu_3N_6O_{13}$	$C_{66}H_{80}Cl_2Cu_6N_{12}O_{17}\cdot 0.5H_2O$
fw	992.26	1774.59
space group	$P2_1/c$ (No. 14)	$P2_1/n$ (No. 14)
a, Å	15.350 (1)	15.622 (2)
b, Å	12.508 (1)	27.025 (2)
c, Å	21.439 (2)	18.864 (4)
β, deg	96.81 (1)	97.38 (2)
V, Å^3	4087.1	7897.9
Z	4	4
T, °C	18	18
ρ_{calcd}, g cm^{-3}	1.61	1.49
μ(Cu Kα), cm^{-1}	36.0	29.4
transm coeff	0.87–0.98	0.74–1.00
$R(F_o)$, $R_w(F_o)$	0.056, 0.05	0.075, 0.091
radiation	graphite-monochromated Cu Kα (λ = 1.5418 Å)	

Preparation of $[Cu_3(\mu_3\text{-}OH)L_3(ClO_4)_2H_2O]$ (1). Stoichiometric amounts of a millimolar methanol–nitromethane (1/1) solution of LH and a millimolar aqueous copper(II) perchlorate solution were mixed, yielding a dark green product. Ethanol was added to avoid phase separation and the solution was slowly evaporated, giving small green black plates suitable for X-ray structure determination. Anal. Calcd for $C_{33}H_{42}Cl_2Cu_3N_6O_{13}$: C, 39.94; H, 4.27; N, 8.47. Found: C, 39.70; H, 4.37; N, 8.40. IR: ν (μ_3(O–H)) = 3470 cm^{-1} (sharp).

Preparation of $[Cu_6(\mu_4\text{-}O)_2L_6(H_2O)](ClO_4)_2\cdot 0.5H_2O$ (2). Thin green plates were obtained by evaporation of a 1:1 mixture of **1** and a base in a methanol–ethanol–nitromethane medium. The bases used were sodium hydroxide, sodium phosphate, and hydrogen phosphates and several mononucleotides as disodium salts. ^{241}Am X-ray fluorescence (Si–Li detector) confirmed that **2** did not contain phosphate groups when phosphate bases were used. Thus no substitution of perchlorate by phosphate occurs under these conditions. Anal. Calcd for $C_{66}H_{81}Cl_2Cu_6N_{12}O_{17.5}$: C, 44.67; H, 4.60; N, 9.47. Found: C, 44.43; H, 4.64; N, 9.41.

X-ray Crystallography. Suitable crystals were sealed in thin-walled Lindemann glass capillaries and mounted on an Enraf-Nonius CAD4 diffractometer equipped with Cu Kα radiation and a graphite monochromator. The data were collected at 18 ± 1 °C, using the ω–2θ scan technique. The net intensities of the data were corrected for Lorentz and polarization effects. No decay was observed. An empirical absorption correction based on a series of ψ-scans was applied to the data.

Both structures were solved by direct methods using the SDP/VAX (Enraf-Nonius) program system.[27] All hydrogen atoms were located from a series of difference Fourier syntheses and included as fixed contributions. The temperature factor of each hydrogen was ca. 30% larger than the equivalent isotropic temperature factor of the corresponding carbon atom. The minimized function was $\sum w(|F_o| - |F_c|)^2$, with the weight w calculated as $w = 4F_o^2/\sigma^2(F_o^2)$ and $\sigma(F_o^2) = [\sigma(I) + (pI)^2]^{1/2}$; $\sigma(I)$ is based on counting statistics and p is an instability factor obtained from plots of F_o vs weighted error.

Crystallographic data are given in Table I. Tables II and III list atomic coordinates, while Table IV gives selected bond distances and angles for **1** and **2**. The atomic scattering factors were taken from the usual source, and the effects of anomalous dispersion were included.[28]

Complex 1. Final cell parameters and the orientation matrix for data collection were obtained from least-squares refinement by using the setting angles of 16 reflections in the range $20 < \theta < 25°$. From a total of 6293 unique reflections ($2 < 2\theta < 120°$, $h = 0$ to 17, $k = 0$ to 14, $l = -24$ to 24), 2986 with $F_o^2 > 3\sigma(F_o^2)$ were used in the full-matrix least-squares procedure. The last cycle of refinement converged to $R = \sum||F_o| - |F_c||/\sum|F_o|$ and $R_w = [\sum w(|F_o| - |F_c|)^2/\sum w|F_o|^2]^{1/2}$ values of 0.056 and 0.057, respectively. A final difference-Fourier map showed

(14) Knuuttila, P. *Inorg. Chim. Acta* **1982**, *58*, 201–206.
(15) Agnus, Y. Thèse Docteur-Ingénieur, Université Louis Pasteur, Strasbourg, France, 1976.
(16) Ross, P. F.; Murmann, R. K.; Schlemper, E. O. *Acta Crystallogr., Sect. B* **1974**, *B30*, 1120–1123.
(17) Baral, S.; Chakravorty, A. *Inorg. Chim. Acta* **1980**, *39*, 1–8.
(18) Chakravorty, A.; Mascharak, P. K.; Datta, D. *Inorg. Chim. Acta* **1978**, *27*, L95–L96.
(19) Datta, D.; Mascharak, P. K.; Chakravorty, A. *Inorg. Chem.* **1981**, *20*, 1673–1679.
(20) Datta, D.; Chakravorty, A. *Inorg. Chem.* **1982**, *21*, 363–368.
(21) Datta, D.; Chakravorty, A. *Inorg. Chem.* **1983**, *22*, 1611–1613.
(22) Mohanty, J. G.; Baral, S.; Singh, R. P.; Chakravorty, A. *Inorg. Nucl. Chem. Lett.* **1974**, *10*, 655–660.
(23) (a) Gruber, S. J.; Harris, C. M.; Sinn, E. *J. Chem. Phys.* **1968**, *49*, 2183–2191. (b) Sinn, E. *Coord. Chem. Rev.* **1970**, *5*, 313–347. (c) Fieselmann, B. F.; Hendrickson, D. N.; Stucky, G. D. *Inorg. Chem.* **1978**, *17*, 1841–1848.
(24) McKee, V.; Tandon, S. S. *J. Chem. Soc., Chem. Commun.* **1988**, 385–387.
(25) McKee, V.; Tandon, S. S. *Inorg. Chem.* **1989**, *28*, 2901–2902.
(26) Uhlig, E.; Friedrich, M. *Z. Anorg. Allg. Chem.* **1966**, *343*, 299–307.
(27) All crystallographic work was done at the Laboratoire de Cristallographie Biologique, IBMC du CNRS, Strasbourg, France. The calculations were carried out on a VAX cluster with SDP: *Structure Determination Package*; Frenz, B. A. & Associates Inc.: College Station, TX, 1983.
(28) (a) Cromer, D. T.; Waber, J. T. *International Tables for X-ray Crystallography*; The Kynoch Press: Birmingham, England, 1974; Vol. IV, Table 2.2B. (b) Cromer, D. T. *International Tables for X-ray Crystallography*; The Kynoch Press: Birmingham, England, 1974, Vol. IV, Table 2.3.1.

Table II. Positional Parameters and Their Estimated Standard Deviations for $[Cu_3(C_{11}H_{13}N_2O)_3(OH)(ClO_4)_2H_2O]$ (1)

atom	x	y	z	B_{eqv},[a] Å^2
Cu1	0.23051 (9)	0.0423 (1)	0.17515 (6)	4.67 (3)
Cu2	0.34893 (8)	−0.1712 (1)	0.18518 (6)	4.30 (3)
Cu3	0.26125 (9)	−0.0897 (1)	0.04814 (6)	4.85 (3)
Cl1	0.1174 (2)	−0.1936 (2)	0.1622 (1)	4.68 (6)
O11	0.1939 (4)	−0.2305 (5)	0.2010 (3)	5.8 (2)
O12	0.0444 (4)	−0.2534 (5)	0.1734 (4)	7.5 (2)
O13	0.1048 (4)	−0.0828 (5)	0.1773 (3)	7.1 (2)
O14	0.1333 (5)	−0.2014 (6)	0.0984 (3)	7.3 (2)
Cl2	0.5817 (2)	−0.1405 (2)	0.1280 (1)	6.99 (8)
O21	0.5113 (5)	−0.0977 (6)	0.1590 (4)	9.7 (2)
O22	0.6556 (5)	−0.0796 (8)	0.1366 (5)	13.4 (3)
O23	0.5980 (7)	−0.2458 (7)	0.1462 (5)	15.0 (4)
O24	0.5494 (8)	−0.1438 (9)	0.0650 (4)	15.8 (4)
O1	0.3117 (4)	−0.0459 (4)	0.1330 (3)	4.1 (1)
O1A	0.3477 (4)	−0.0890 (5)	0.2614 (3)	4.7 (2)
N2A	0.2909 (4)	−0.0083 (5)	0.2554 (3)	4.1 (2)
C3A	0.2728 (6)	0.0414 (7)	0.3044 (4)	4.4 (2)
C4A	0.3144 (7)	0.0161 (8)	0.3690 (5)	6.0 (3)
C5A	0.2061 (6)	0.1260 (7)	0.2906 (4)	4.5 (2)
C6A	0.1783 (7)	0.1885 (8)	0.3446 (5)	7.0 (3)
N7A	0.1764 (5)	0.1387 (5)	0.2321 (4)	4.7 (2)
C8A	0.1035 (6)	0.2153 (7)	0.2111 (4)	4.9 (2)
C9A	0.1371 (6)	0.3205 (7)	0.1885 (5)	5.3 (3)
C10A	0.1595 (9)	0.4014 (9)	0.2289 (5)	9.1 (4)
C11A	0.188 (1)	0.4985 (9)	0.2076 (6)	10.2 (4)
C12A	0.1929 (7)	0.5154 (8)	0.1469 (6)	7.4 (3)
C13A	0.1722 (7)	0.4356 (8)	0.1053 (5)	7.2 (3)
C14A	0.1438 (7)	0.3376 (8)	0.1266 (5)	6.9 (3)
O1B	0.3272 (4)	−0.2221 (5)	0.0510 (3)	4.9 (2)
N2B	0.3530 (4)	−0.2567 (5)	0.1081 (3)	4.0 (2)
C3B	0.3909 (6)	−0.3485 (7)	0.1167 (4)	4.6 (2)
C4B	0.4080 (7)	−0.4189 (8)	0.0622 (5)	6.8 (3)
C5B	0.4109 (5)	−0.3774 (7)	0.1832 (4)	4.5 (2)
C6B	0.4452 (7)	−0.4871 (8)	0.1995 (5)	6.8 (3)
N7B	0.3923 (4)	−0.3074 (5)	0.2232 (3)	4.1 (2)
C8B	0.3960 (6)	−0.3281 (7)	0.2909 (4)	5.2 (3)
C9B	0.4820 (6)	−0.2945 (7)	0.3284 (4)	4.2 (2)
C10B	0.4848 (6)	−0.278 (1)	0.3922 (4)	7.6 (3)
C11B	0.5622 (7)	−0.252 (1)	0.4284 (5)	8.5 (4)
C12B	0.6372 (7)	−0.2424 (9)	0.4009 (5)	7.0 (3)
C13B	0.6344 (6)	−0.2560 (8)	0.3386 (5)	6.2 (3)
C14B	0.5575 (6)	−0.2817 (7)	0.3018 (4)	5.0 (3)
O1C	0.1689 (4)	0.0925 (5)	0.0967 (3)	5.1 (2)
N2C	0.1789 (4)	0.0313 (6)	0.0479 (3)	4.4 (2)
C3C	0.1302 (6)	0.0458 (7)	−0.0048 (4)	5.2 (3)
C4C	0.0629 (7)	0.1336 (9)	−0.0147 (5)	7.9 (3)
C5C	0.1463 (6)	−0.0318 (8)	−0.0537 (4)	5.0 (2)
C6C	0.0962 (8)	−0.019 (1)	−0.1175 (5)	8.4 (4)
N7C	0.2024 (5)	−0.1043 (6)	−0.0379 (3)	4.9 (2)
C8C	0.2291 (6)	−0.1853 (9)	−0.0819 (4)	5.9 (3)
C9C	0.1658 (6)	−0.2787 (7)	−0.0915 (4)	4.9 (2)
C10C	0.1366 (7)	−0.3307 (9)	−0.0406 (4)	6.4 (3)
C11C	0.0831 (7)	−0.4190 (9)	−0.0490 (5)	7.5 (3)
C12C	0.0563 (7)	−0.456 (1)	−0.1093 (5)	8.3 (4)
C13C	0.0848 (7)	−0.4053 (9)	−0.1593 (5)	7.6 (3)
C14C	0.1377 (7)	−0.3153 (9)	−0.1515 (5)	7.3 (3)
O2	0.3913 (5)	−0.0103 (6)	0.0200 (4)	10.0 (3)

[a] Values for anisotropically refined atoms are given in the form of the isotropic equivalent displacement parameter defined as $(4/3)[a^2B(1,1) + b^2B(2,2) + c^2B(3,3) + ab(\cos\gamma)B(1,2) + ac(\cos\beta)B(1,3) + bc(\cos\alpha)B(2,3)]$.

no significant features with the highest peak at 0.49 e Å^{-3}. All non-hydrogen atoms were refined anisotropically.

Complex 2. Unit cell parameters and the orientation matrix for data collection were determined from the setting angles of 16 reflections in the range $19 < \theta < 21°$, measured by the computer-controlled diagonal slit method of centering. Data were collected in the range $2 < 2\theta < 108°$ ($h = -17$ to $+17$, $k = 0$ to 29, $l = 0$ to 20). Only 3453 from a total of 9638 unique reflections having intensities $F_o^2 > 3\sigma(F_o^2)$ were used in the refinement. A secondary extinction correction was applied.[29] The final R and R_w values are equal to 0.075 and 0.091, respectively. The highest peak on the final difference-Fourier synthesis was at 0.79 e Å^{-3}. The

(29) Zachariasen, W. H. *Acta Crystallogr.* **1963**, *16*, 1139–1144.

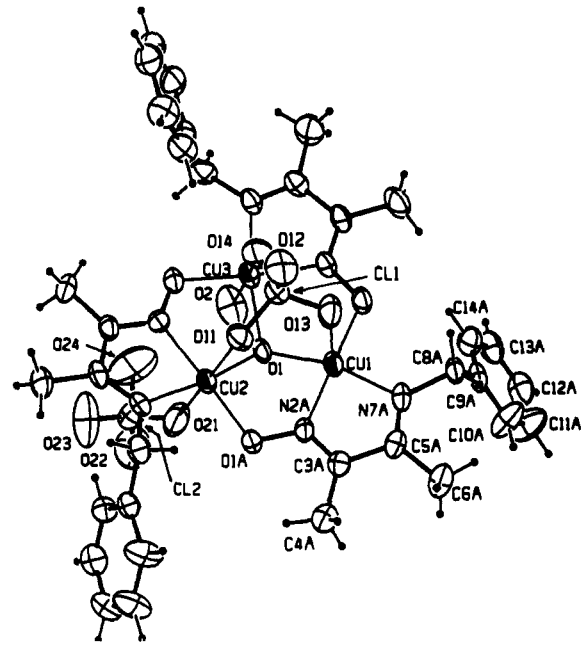

Figure 1. ORTEP drawing of $[Cu_3(\mu_3\text{-}OH)L_3(ClO_4)_2(H_2O)]$ (1), showing 30% probability ellipsoids and the atom-labeling scheme. The labels B and C of the oximato ligands are omitted for clarity.

non-hydrogen atoms, except the carbon atoms and the oxygen atoms of the two water molecules, were refined anisotropically.

Electrochemical Experiments. The electrochemical experiments were carried out in propylene carbonate (PC) purified as described previously[30a] and stored under argon. Tetrabutylammonium perchlorate (TBAP) from Fluka was used as supporting electrolyte in PC and recrystallized before use.[30b] Cyclic voltammetry experiments, with scan rates ranging from 10 to 20 V/s on Pt electrodes, were carried out on a multipurpose computerized device, Dacfamov (Microtec-CNRS, Toulouse, France), connected to an Apple II computer. The working electrode was a Pt disk electrode (2 mm diameter from Tacussel, EDI type). The reference electrode was a saturated calomel electrode (SCE), and the auxiliary electrode was a Pt wire. Ferrocene was used as an internal reference throughout the set of experiments. It was oxidized reversibly at +0.37 V versus SCE in our experimental conditions. The supporting electrolyte solutions were deoxygenated by an argon stream for at least 5 min before introduction of the studied compounds. Furthermore, they were protected from air by argon flowing over the solution during the experiment.

Results and Discussion

Complex **1** is represented in Figure 1. The central core is composed of the hydroxo group O1 slightly below (0.60 (1) Å) the plane of the three copper ions {3Cu}. The values of the bonding Cu–O1 distances are equivalent and equal to 1.963 (6), 1.971 (5), and 1.968 (5) Å. The metal ions lie at the corners of an equilateral triangle and are at an average distance of 3.245 (2) Å from each other. An imine nitrogen atom and the oximato N–O end-to-end bridging fragment of three L^- moieties compose with the μ_3-hydroxo ion three equatorial square arrangements, denoted as {Cu1}, {Cu2}, and {Cu3}. The dihedral angles between the plane {3Cu} and mean planes {Cu1}, {Cu2}, and {Cu3} are equal to 13.4 (2), 17.8 (1), and 16.4 (1)°, respectively.

Each copper ion also interacts with axial donor atoms. The three axial positions above the plane {3Cu} are occupied by three oxygen atoms of a "tripodal" perchlorate. The corresponding copper–oxygen bonds are not alike: two medium copper–oxygen distances and one long copper–oxygen distance are observed, Cu1–O13 = 2.489 (7) Å, Cu2–O11 = 2.553 (6) Å, and Cu3–O14 = 2.734 (7) Å. The Cu1–O13 bond is the shortest, because Cu1 does not possess a second axial ligand. Cu2 and Cu3 interact with respectively an oxygen atom of the second perchlorate ion and a water molecule denoted as O2. The observed distances are

(30) (a) Ritzler, G.; Peter, F.; Gross, M. *J. Electroanal. Chem. Interfacial Electrochem.* **1983**, *146*, 285–301. (b) El Jammal, A.; Graf, E.; Gross, M. *J. Electroanal. Chem. Interfacial Electrochem.* **1986**, *214*, 507–517.

Table III. Positional Parameters for $[Cu_6(C_{11}H_{13}N_2O)_6(O)_2(H_2O)](ClO_4)_2 \cdot 0.5H_2O$ (**2**)

atom	x	y	z	B_{eqv},[a] Å^2	atom	x	y	z	B_{eqv},[a] Å^2
Cu1	0.8931 (2)	0.3747 (1)	0.7710 (2)	3.73 (7)	C3D	0.629 (1)	0.3939 (7)	0.603 (1)	3.2 (4)*
Cu2	1.0138 (2)	0.2907 (1)	0.8461 (2)	3.85 (8)	C4D	0.540 (1)	0.3971 (8)	0.625 (1)	4.4 (5)*
Cu3	1.0958 (2)	0.3737 (1)	0.7573 (2)	3.91 (7)	C5D	0.662 (1)	0.4263 (7)	0.551 (1)	3.6 (5)*
Cu4	0.8022 (2)	0.3691 (1)	0.6028 (2)	3.41 (7)	C6D	0.597 (1)	0.4618 (9)	0.509 (1)	5.8 (6)*
Cu5	0.7613 (2)	0.2823 (1)	0.7057 (2)	3.54 (7)	N7D	0.7397 (9)	0.4219 (6)	0.5427 (8)	3.6 (4)
Cu6	0.9548 (2)	0.2978 (1)	0.6715 (2)	3.62 (7)	C8D	0.782 (1)	0.4493 (8)	0.491 (1)	4.4 (5)*
O1	0.9961 (7)	0.3392 (5)	0.7749 (7)	3.7 (3)	C9D	0.786 (1)	0.4216 (8)	0.422 (1)	4.4 (5)*
O2	0.8417 (7)	0.3231 (4)	0.6720 (6)	3.1 (3)	C10D	0.726 (1)	0.3882 (9)	0.396 (1)	6.4 (7)*
O1A	1.0306 (7)	0.4301 (5)	0.7139 (8)	4.9 (4)	C11D	0.731 (2)	0.364 (1)	0.330 (1)	7.4 (7)*
N2A	0.9503 (9)	0.4301 (6)	0.7273 (9)	3.8 (4)	C12D	0.793 (2)	0.375 (1)	0.290 (1)	8.8 (8)*
C3A	0.901 (1)	0.4676 (8)	0.709 (1)	4.2 (5)*	C13D	0.851 (2)	0.409 (1)	0.318 (1)	9.0 (8)*
C4A	0.933 (1)	0.5130 (9)	0.672 (1)	6.8 (7)*	C14D	0.848 (1)	0.4322 (9)	0.380 (1)	6.6 (6)*
C5A	0.815 (1)	0.4642 (8)	0.731 (1)	4.3 (5)*	O1E	0.9341 (8)	0.2392 (5)	0.7292 (7)	4.3 (4)
C6A	0.749 (1)	0.5067 (8)	0.716 (1)	5.5 (6)*	N2E	0.8509 (9)	0.2318 (6)	0.7341 (9)	4.1 (4)
N7A	0.7979 (9)	0.4246 (6)	0.7640 (8)	3.7 (4)	C3E	0.823 (1)	0.1920 (7)	0.756 (1)	3.7 (5)*
C8A	0.714 (1)	0.4172 (8)	0.793 (1)	4.2 (5)*	C4E	0.884 (1)	0.1484 (8)	0.779 (1)	5.7 (6)*
C9A	0.705 (1)	0.4492 (8)	0.856 (1)	4.9 (5)*	C5E	0.727 (1)	0.1899 (7)	0.754 (1)	2.9 (4)*
C10A	0.770 (2)	0.4557 (9)	0.912 (1)	7.3 (7)*	C6E	0.688 (1)	0.1408 (8)	0.772 (1)	5.4 (6)*
C11A	0.754 (2)	0.490 (1)	0.969 (2)	12 (1)*	N7E	0.6858 (9)	0.2289 (5)	0.7357 (9)	3.8 (4)
C12A	0.679 (2)	0.511 (1)	0.967 (2)	9.9 (9)*	C8E	0.590 (1)	0.2306 (7)	0.728 (1)	4.0 (5)*
C13A	0.619 (2)	0.506 (1)	0.916 (2)	9.9 (9)*	C9E	0.559 (1)	0.2399 (8)	0.799 (1)	4.3 (5)*
C14A	0.626 (1)	0.4738 (9)	0.857 (1)	6.9 (7)*	C10E	0.578 (2)	0.284 (1)	0.831 (1)	8.4 (8)*
O1B	0.8378 (7)	0.3285 (5)	0.8322 (6)	3.5 (3)	C11E	0.549 (2)	0.290 (1)	0.901 (1)	8.8 (8)*
N2B	0.8984 (9)	0.2994 (6)	0.8700 (8)	3.5 (4)	C12E	0.509 (2)	0.252 (1)	0.926 (1)	8.3 (8)*
C3B	0.876 (1)	0.2759 (7)	0.922 (1)	3.6 (5)*	C13E	0.483 (2)	0.212 (1)	0.899 (2)	9.5 (8)*
C4B	0.787 (1)	0.2765 (9)	0.945 (1)	5.8 (6)*	C14E	0.511 (2)	0.206 (1)	0.830 (1)	7.5 (7)*
C5B	0.948 (1)	0.2471 (7)	0.959 (1)	3.6 (5)*	O1F	0.9130 (7)	0.3791 (5)	0.5695 (7)	4.0 (3)
C6B	0.938 (1)	0.2245 (8)	1.028 (1)	5.6 (6)*	N2F	0.9704 (8)	0.3459 (5)	0.5941 (8)	2.8 (4)
N7B	1.0154 (9)	0.2455 (6)	0.9304 (8)	4.4 (5)	C3F	1.043 (1)	0.3452 (7)	0.572 (1)	3.4 (5)*
C8B	1.094 (1)	0.2214 (9)	0.960 (1)	5.9 (6)*	C4F	1.069 (1)	0.3821 (8)	0.521 (1)	4.8 (5)*
C9B	1.154 (1)	0.2574 (8)	1.000 (1)	5.1 (6)*	C5F	1.099 (1)	0.3045 (7)	0.600 (1)	3.7 (5)*
C10B	1.243 (2)	0.245 (1)	1.007 (1)	8.1 (8)*	C6F	1.188 (1)	0.2964 (9)	0.576 (1)	5.9 (6)*
C11B	1.303 (2)	0.279 (1)	1.045 (2)	9.5 (8)*	N7F	1.0695 (8)	0.2767 (6)	0.6463 (8)	3.5 (4)
C12B	1.276 (2)	0.323 (1)	1.068 (2)	10.6 (9)*	C8F	1.116 (1)	0.2312 (8)	0.677 (1)	4.3 (5)*
C13B	1.190 (2)	0.337 (1)	1.066 (2)	11 (1)*	C9F	1.101 (1)	0.1878 (7)	0.627 (1)	3.5 (5)*
C14B	1.135 (2)	0.301 (1)	1.030 (1)	7.4 (7)*	C10F	1.021 (1)	0.1690 (8)	0.609 (1)	5.2 (6)*
O1C	1.1358 (7)	0.2807 (5)	0.8361 (7)	4.1 (4)	C11F	1.005 (1)	0.1296 (9)	0.560 (1)	6.8 (7)*
N2C	1.1636 (9)	0.3166 (6)	0.7972 (8)	3.8 (4)	C12F	1.074 (1)	0.1085 (9)	0.531 (1)	7.0 (7)*
C3C	1.244 (1)	0.3172 (8)	0.787 (1)	4.3 (5)*	C13F	1.155 (1)	0.1263 (9)	0.551 (1)	6.2 (6)*
C4C	1.307 (1)	0.2773 (9)	0.815 (1)	5.8 (6)*	C14F	1.170 (1)	0.1650 (8)	0.598 (1)	5.0 (6)*
C5C	1.265 (1)	0.3593 (7)	0.745 (1)	3.3 (5)*	Cl1	1.3204 (4)	0.4004 (2)	0.4676 (3)	5.8 (2)
C6C	1.355 (1)	0.3610 (8)	0.722 (1)	5.7 (6)*	Cl2	0.9253 (5)	0.3705 (4)	1.1151 (5)	12.3 (3)
N7C	1.2081 (9)	0.3911 (6)	0.7250 (8)	3.9 (4)	O11	1.331 (1)	0.4008 (8)	0.5406 (8)	10.3 (6)
C8C	1.225 (1)	0.4349 (8)	0.684 (1)	4.4 (5)*	O12	1.399 (1)	0.4096 (8)	0.445 (1)	12.1 (7)
C9C	1.287 (1)	0.4725 (8)	0.722 (1)	4.5 (5)*	O13	1.262 (1)	0.4352 (7)	0.442 (1)	12.5 (7)
C10C	1.356 (1)	0.4883 (8)	0.690 (1)	5.4 (6)*	O14	1.288 (1)	0.3543 (6)	0.4408 (9)	8.8 (5)
C11C	1.417 (2)	0.524 (1)	0.722 (1)	8.5 (8)*	O21	0.891 (2)	0.322 (1)	1.141 (1)	19 (1)
C12C	1.403 (2)	0.538 (1)	0.788 (1)	8.6 (8)*	O22	1.006 (1)	0.388 (1)	1.154 (2)	23 (1)
C13C	1.339 (2)	0.525 (1)	0.820 (2)	14 (1)*	O23	0.870 (2)	0.4085 (9)	1.119 (1)	20 (1)
C14C	1.281 (2)	0.490 (1)	0.788 (2)	9.7 (9)*	O24	0.938 (2)	0.363 (1)	1.050 (1)	25 (1)
O1D	0.6648 (7)	0.3270 (5)	0.6751 (7)	3.7 (3)	OA	1.132 (2)	0.415 (1)	0.879 (1)	17.2 (9)*
N2D	0.6840 (9)	0.3604 (5)	0.6291 (8)	3.1 (4)	OB	1.007 (4)	0.437 (2)	0.949 (3)	20 (2)*

[a] Starred values denote atoms that were refined isotropically. Values for anisotropically refined atoms are given in the form of the isotropic equivalent displacement parameter defined as $(4/3)[a^2B(1,1) + b^2B(2,2) + c^2B(3,3) + ab(\cos\gamma)B(1,2) + ac(\cos\beta)B(1,3) + bc(\cos\alpha)B(2,3)]$.

Cu2–O21 = 2.777 (8) Å and Cu3–O2 = 2.372 (8) Å. The Cu–O interactions observed here are within the known range.[24] Thus Cu2 and Cu3 are six-coordinate; the corresponding octahedra are highly distorted each with a medium and a weak axial interaction. Cu1 presents a square-pyramidal environment with a moderate apical interaction. The observed Cl–O distances in the perchlorate ions reflect the coordination to copper. Thus, Cl1–O11, Cl1–O13, Cl1–O14, and Cl2–O21 (1.433 (6), 1.442 (7), 1.421 (7) and 1.437 (9) Å, respectively) are longer than the chlorine–noncoordinating oxygen distances (1.391 (7), 1.361 (9), 1.39 (1), and 1.383 (8) Å). The benzyl groups of the three L^- moieties are pointing outside the central core: two below and one above the plane {3Cu}.

Figure 2 shows the copper stereochemistries with the atom-labeling scheme in complex **2**. **2** consists of two linked $[Cu_3OL_3]^+$ units. Here two oxo ions behave as μ_4-bridging ligands: each oxo ion bridges three coppers of one unit and one copper of the other. The average value of the Cu···Cu distances in the two {3Cu} planes is 3.185 (4) Å, slightly smaller than that in **1**. Each trinuclear unit is completed by three L^- moieties. Nonchelating perchlorate ions assume the charge balance. Two water molecules OA and OB are also present in the asymmetric unit, with OB occupying its position only about half of the time. The Cu2, Cu4, and Cu5 ions have square-planar stereochemistries, with the donor atoms of L^- in the equatorial planes as found for **1**. Cu1, Cu3, and Cu6 have square-pyramidal environments. The apical positions are occupied by the μ_4-oxo ligands for Cu1 (Cu1–O2 = 2.38 (1) Å) and Cu6 (Cu6–O1 = 2.29 (1) Å) and by the water molecule OA for Cu3 (Cu3–OA = 2.55 (3) Å). These apical interactions are moderately strong for copper(II) ions.

The two {3Cu} planes are nearly parallel with a mean separation of 2.7 Å and a dihedral angle of 4 (1)°. The bridging Cu_2O_2 core is folded. The value of the dihedral angle between the {Cu1,Cu6,O1} and {Cu1,Cu6,O2} planes is equal to 12 (2)°. The oxo ligands are located closer to the {3Cu} planes (0.35 (1) for O1 and 0.29 (1) Å for O2) than the hydroxide ion in **1**. The Cu–oxo bonds are also shorter (1.85 (1)–1.89 (1) Å). These observations are in agreement with those reported in similar triangular copper(II) systems.[4-6,8-10,12,13,16] The triangular Cu_3

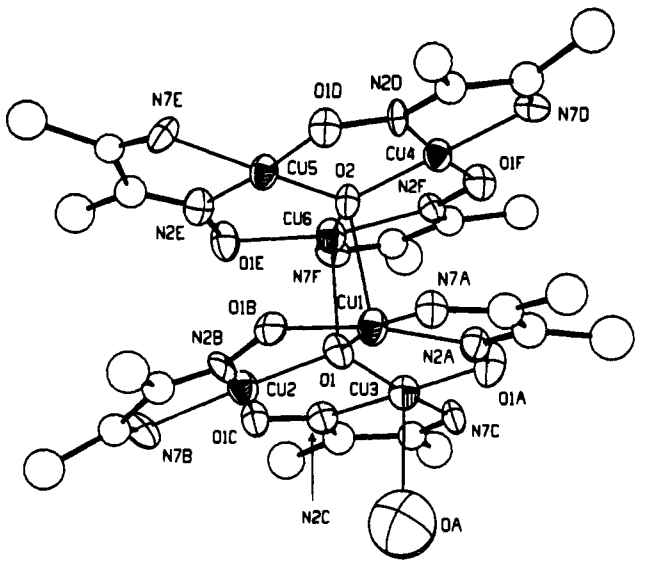

Figure 2. View of the copper stereochemistries in the $[Cu_6(\mu_4\text{-}O)_2L_6(H_2O)]^{2+}$ cation present in **2** with the atom-numbering scheme. The thermal ellipsoids are drawn at 40% probability.

core appears particularly well designed to give axial interactions with oxygen atoms of tetrahedral oxoanions. Such arrangements are known for sulfato[4,15,31,32] and phosphato[15,32-34] complexes. Recently a tridentate bridging perchlorate anion has been observed in a square Cu_4 core.[25] However the corresponding Cu–O distances are longer than in **1** owing to the unfavorable topological matching between square Cu_4 and tetrahedral ClO_4^- geometries. Tridentate coordination of ClO_4^- in nickel and cobalt perchlorates has been suggested on the basis of EXAFS studies.[35]

The comparison of IR spectra of **1** and **2** allows their direct identification. Actually, in both compounds the stretching modes ν_1 and ν_3 of the water molecules give the classical broad band in the 3200–3800-cm^{-1} region, but in **1**, this broad band is overreached by a sharp and strong peak at 3470 cm^{-1}, due to the O–H stretching mode of the μ_3-hydroxo ion. The mono- and tridentate perchlorate ions in **1** have both C_{3v} symmetry, resulting in the increase of vibration modes with respect to those in the tetrahedral ion.[36-38] The corresponding frequencies are observed: 1120 (strong, ν_4), 1060 (moderately strong, ν_1), 635–615 (medium with shoulder, $\nu_3 + \nu_5$), 465 (medium, ν_6), and 920 cm^{-1} (weak, ν_2). In **2**, the perchlorate ions are uncoordinated; the observed frequencies 1115–1090 (strong, ν_3) and 620 cm^{-1} (medium, ν_4) agree with the IR-active normal modes for T_d symmetry.

Complex **1** is characterized by two reduction waves at $E_{1/2}$ = −0.41 and about −1.00 V versus SCE (Pt rotating disk electrode = RDE) (Figure 3a). The second step is ill-defined due to strong inhibition of the Pt electrode surface. The first reduction wave exhibits characteristics (60 mV/(log unit) from E versus log $(I/(I_d - I))$ plots) of a reversible one-electron charge transfer to the Cu_3 core. Cyclic voltammetry between +0.80 and −1.50 V versus SCE shows two well-defined irreversible reduction peaks at −0.46 and −1.07 V versus SCE (Figure 4a) and an anodic peak at −0.31 V versus SCE. This peak is only observed when the potentials beyond more negative values than −0.80 V versus SCE are scanned, and it therefore does not correspond to the oxidation of the species

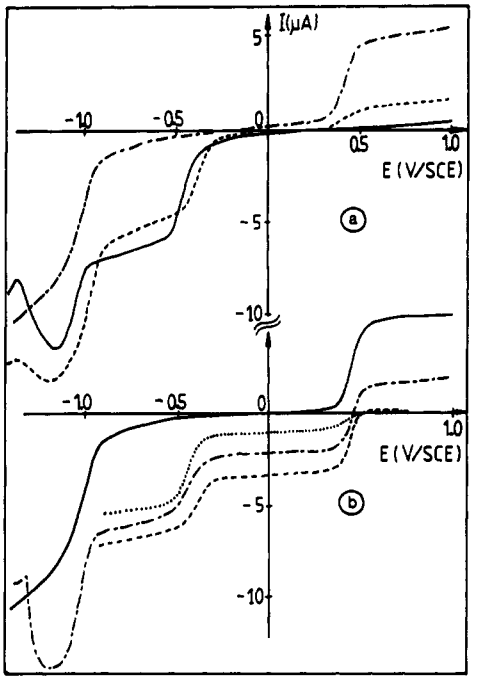

Figure 3. Voltammograms of **1** and **2**, in PC + 0.1 M TBAP on platinum RDE: (a) **1** in solution (denoted $[Cu^{II}_3(OH)]^{2+}$), $c = 1.2 \times 10^{-3}$ M (—); **1** after reduction at −0.70 V versus SCE (-·-); **1** after reduction at −0.70 V versus SCE and reoxidation at +0.70 V versus SCE (--); (b) **2** in solution (denoted $[Cu^{II}_3(O)]^+$), $c = 5.3 \times 10^{-4}$ M (—); **2** after 80% oxidation at +0.70 V versus SCE (-·-); **2** after exhaustive oxidation at +0.70 V versus SCE (--); oxidized solution after 48 hours (···).

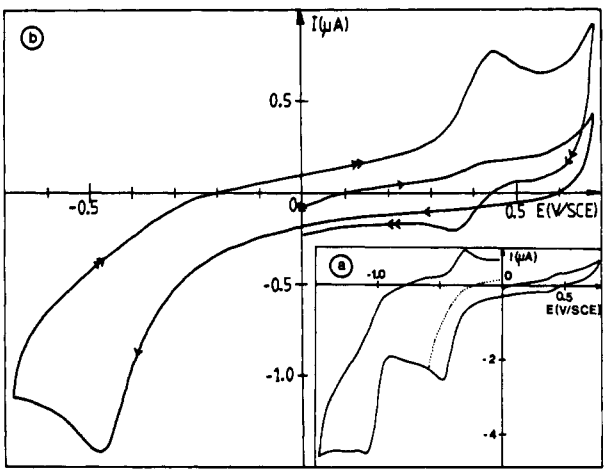

Figure 4. Cyclic voltammograms of **1** on platinum at $v = 100$ mV s^{-1} in PC + 0.1 M TBAP: (a) $c = 9.9 \times 10^{-4}$ M (dotted line; cyclic voltammetry from +0.80 to −0.60 V versus SCE), with the small amplitude redox couple observed at 0.42 V versus SCE being due to contamination of **1** by a small amount of **2**; (b) $c = 5.4 \times 10^{-4}$ M.

electrogenerated at −0.46 V versus SCE. In the first reduction step, the dependence of the reduction peak parameters to the scan rate is typical of an EC mechanism (reversible monoelectronic charge transfer followed by a fast irreversible chemical step). Cyclic voltammetry initiated at 0.0 V toward positive potentials shows, surprisingly, after the first cathodic scan down to −0.70 V, the growth of a reversible monoelectronic step at $E°$ = +0.42 V versus SCE (Figure 4b) corresponding to a Cu(II)/Cu(I) couple, the nature of which will be discussed later.

On RDE, **2** shows one oxidation wave at $E_{1/2}$ = +0.42 V versus SCE and one reduction wave at −1.07 V versus SCE per trinuclear subunit (Figure 3b). The oxidation step is monoelectronic and reversible and corresponds to the couple **2**/**4**, $[Cu(II)_3O]^+/[Cu(III)Cu(II)_2O]^{2+}$. By cyclic voltammetry between +1.40 and −1.50 V versus SCE at 0.10 V/s, **2** exhibits a well-defined reversible one-electron oxidation at $E°$ = +0.42 V versus SCE and

(31) Estienne, J.; Weiss, R. *J. Chem. Soc., Chem. Commun.* **1972**, 862–863.
(32) Keiter, R. L.; Strickland, D. S.; Wilson, S. R.; Shapley, J. R. *J. Am. Chem. Soc.* **1986**, *108*, 3846–3847.
(33) Troup, J. M.; Clearfield, A. *Inorg. Chem.* **1977**, *16*, 3311–3314.
(34) Torardi, C. C.; Calabrese, J. C. *Inorg. Chem.* **1984**, *23*, 1308–1310.
(35) Pascal, J. L.; Potier, J.; Jones, D. J.; Rozière, J.; Michalowicz, A. *Inorg. Chem.* **1985**, *24*, 238–241.
(36) Nakamoto, K. *Infrared and Raman Spectra of Inorganic and Coordination Compounds*, 4th ed.; Wiley-Interscience: New York, 1986.
(37) Hathaway, B. J.; Underhill, A. E. *J. Chem. Soc.* **1961**, 3091–3096.
(38) Gowda, N. M. N.; Naikar, S. B.; Reddy, G. K. N. *Adv. Inorg. Chem. Radiochem.* **1984**, *28*, 255–299.

Table IV. Selected Distances (Å) and Angles (deg) for **1** and **2**[a]

		Distances in **1**			
Cu1–O13	2.489 (7)	Cu2–O1A	1.933 (6)	Cu3–O1B	1.938 (6)
Cu1–O1	1.963 (6)	Cu2–O21	2.777 (8)	Cu3–N2C	1.972 (8)
Cu1–N2A	1.961 (7)	Cu2–N2B	1.974 (7)	Cu3–N7C	1.964 (7)
Cu1–N7A	1.969 (7)	Cu2–O1	1.971 (5)	Cu3–O2	2.372 (8)
Cu1–O1C	1.933 (6)	Cu2–N7B	1.970 (7)	Cu3–O1	1.968 (5)
Cu2–O11	2.553 (6)	Cu3–O14	2.734 (7)		
		Angles in **1**			
O13–Cu1–O1	101.0 (2)	O11–Cu2–N7B	88.3 (2)	O14–Cu3–N7C	93.0 (3)
O13–Cu1–N2A	93.9 (3)	O21–Cu2–O1	80.1 (2)	O14–Cu3–O2	168.6 (2)
O13–Cu1–N7A	89.3 (3)	O21–Cu2–O1A	95.4 (2)	O1–Cu3–O1B	93.5 (2)
O13–Cu1–O1C	85.4 (2)	O21–Cu2–N2B	83.9 (3)	O1–Cu3–N2C	88.3 (3)
O1–Cu1–N2A	87.9 (3)	O21–Cu2–N7B	95.9 (2)	O1–Cu3–N7C	168.7 (3)
O1–Cu1–N7A	165.3 (3)	O1–Cu2–O1A	91.5 (2)	O1–Cu3–O2	82.4 (3)
O1–Cu1–O1C	93.1 (2)	O1–Cu2–N2B	89.5 (2)	O1B–Cu3–N2C	171.3 (3)
N2A–Cu1–N7A	81.0 (3)	O1–Cu2–N7B	169.6 (3)	O1B–Cu3–N7C	97.5 (3)
N2A–Cu1–O1C	179.0 (3)	O1A–Cu2–N2B	178.6 (3)	O1B–Cu3–O2	85.0 (3)
N7A–Cu1–O1C	98.2 (3)	O1A–Cu2–N7B	98.5 (3)	N2C–Cu3–N7C	81.2 (3)
O11–Cu2–O21	175.2 (2)	N2B–Cu2–N7B	80.6 (3)	N2C–Cu3–O2	103.7 (3)
O11–Cu2–O1	95.4 (2)	O14–Cu3–O1	90.0 (2)	N7C–Cu3–O2	96.2 (3)
O11–Cu2–O1A	86.5 (2)	O14–Cu3–O1B	87.0 (2)	Cu1–O1–Cu2	110.0 (3)
O11–Cu2–N2B	94.4 (2)	O14–Cu3–N2C	84.5 (3)	Cu1–O1–Cu3	112.4 (3)
Cu2–O1–Cu3	111.0 (3)				
		Distances in **2**			
Cu1–O1	1.87 (1)	Cu3–O1	1.89 (1)	Cu5–O2	1.85 (1)
Cu1–O2	2.39 (1)	Cu3–N2C	1.97 (2)	Cu5–N2E	1.98 (2)
Cu1–N2A	1.98 (2)	Cu3–N7C	1.99 (2)	Cu5–N7E	1.99 (2)
Cu1–N7A	2.00 (1)	Cu3–O1A	1.95 (1)	Cu5–O1D	1.97 (1)
Cu1–O1B	1.97 (1)	Cu3–OA	2.55 (3)	Cu6–O1	2.27 (1)
Cu2–O1	1.87 (1)	Cu4–O2	1.86 (1)	Cu6–O2	1.89 (1)
Cu2–N2B	1.93 (1)	Cu4–N2D	1.99 (1)	Cu6–N2F	2.00 (1)
Cu2–N7B	2.00 (2)	Cu4–N7D	2.00 (1)	Cu6–N7F	2.00 (1)
Cu2–O1C	1.96 (1)	Cu4–O1F	1.93 (1)	Cu6–O1E	1.97 (1)
		Angles in **2**			
O1–Cu1–O2	86.0 (5)	O1–Cu3–O1A	93.6 (6)	O2–Cu5–O1D	93.5 (6)
O1–Cu1–N2A	88.5 (6)	O1–Cu3–N2C	87.8 (6)	O2–Cu5–N2E	90.9 (6)
O1–Cu1–N7A	168.5 (6)	O1–Cu3–N7C	162.8 (7)	O2–Cu5–N7E	170.2 (6)
O1–Cu1–O1B	95.3 (5)	O1–Cu3–OA	98.8 (7)	O1D–Cu5–N2E	174.4 (6)
O2–Cu1–N2A	103.9 (6)	O1A–Cu3–N2C	177.6 (7)	O1D–Cu5–N7E	94.0 (5)
O2–Cu1–N7A	99.8 (6)	O1A–Cu3–N7C	97.0 (6)	N2E–Cu5–N7E	81.2 (6)
O2–Cu1–O1B	87.6 (5)	O1A–Cu3–OA	94.7 (7)	O1–Cu6–O2	88.9 (5)
N2A–Cu1–N7A	80.5 (6)	N2C–Cu3–N7C	81.4 (6)	O1–Cu6–O1E	88.3 (5)
N2A–Cu1–O1B	168.2 (7)	N2C–Cu3–OA	87.1 (8)	O1–Cu6–N2F	105.0 (5)
N7A–Cu1–O1B	95.0 (6)	N7C–Cu3–OA	93.9 (7)	O1–Cu6–N7F	100.5 (6)
O1–Cu2–N2B	91.5 (6)	O2–Cu4–N2D	88.9 (5)	O2–Cu6–O1E	93.9 (5)
O1–Cu2–N7B	169.2 (7)	O2–Cu4–N7D	167.2 (7)	O2–Cu6–N2F	88.2 (5)
O1–Cu2–O1C	94.8 (5)	O2–Cu4–O1F	95.2 (5)	O2–Cu6–N7F	166.0 (6)
N2B–Cu2–N7B	78.8 (7)	N2D–Cu4–N7D	79.9 (6)	O1E–Cu6–N2F	166.6 (6)
N2B–Cu2–O1C	172.1 (6)	N2D–Cu4–O1F	175.4 (6)	O1E–Cu6–N7F	96.8 (6)
N7B–Cu2–O1C	94.6 (6)	N7D–Cu4–O1F	96.2 (6)	N2F–Cu6–N7F	79.2 (6)
Cu1–O1–Cu2	115.8 (6)	Cu1–O1–Cu3	117.8 (7)	Cu1–O1–Cu6	94.1 (5)
Cu2–O1–Cu3	115.1 (5)	Cu2–O1–Cu6	105.8 (6)	Cu3–O1–Cu6	104.2 (6)
Cu1–O2–Cu4	101.9 (5)	Cu1–O2–Cu5	104.7 (6)	Cu1–O2–Cu6	89.7 (4)
Cu4–O2–Cu5	117.7 (6)	Cu4–O2–Cu6	117.8 (6)	Cu5–O2–Cu6	117.6 (6)

[a] Numbers in parentheses are estimated standard deviations in the least significant digits.

an irreversible reduction peak at −1.07 V versus SCE.

The addition of $HClO_4$ to **2** easily gives **1**, which in turn, by addition of NEt_3 is reverted to **2**. This interconversion has been monitored through electrochemical and spectrophotometric experiments. It has been observed by cyclic voltammetry that the peak current associated with the reversible oxidation of **2** at +0.42 V versus SCE decreases upon addition of $HClO_4$ and vanishes as soon as 1 equiv of $HClO_4$ is added to the solution. Simultaneously, the reduction peak current at −0.46 V versus SCE characteristic of **1** increases up to a maximum constant value. Addition of NEt_3 to the latter solution fully regenerates **2** after addition of 1 equiv of the base (Figure 5). This conversion has been repeated several times as was observed previously on similar compounds.[19,20,25]

Spectroscopically, the **1** ↔ **2** interconversion has been operated over more than three cycles without a noticeable change in the optical densities. UV–visible spectra in PC solution show absorption bands (ϵ in L mol^{-1} cm^{-1}) for **1** at 620 (570), 311 (22450), 240 (20380), and 205 nm (34530) and for **2** at 650 (315), 311 (21500), and 257 nm (23800). Both **1** and **2** are therefore chemically stable species under our operating conditions even if **2** is split into two tricopper–oxo entities.[39]

Exhaustive coulometric oxidation of **2** at +0.70 V versus SCE gives, after a one-electron exchange, a solution containing mainly **4** as shown on RDE by its reduction wave at +0.42 V (Figure 3b) and its characteristic absorption bands in the electronic spectroscopy at 413, 690, and 820 nm (Figure 6). A part of **4** transforms into **1** by a homogeneous chemical reaction evidenced by the occurrence of a second reduction wave at −0.40 V versus

(39) The similarity of the copper stereochemistries in **1** and **2**, implying that **2** is dissociated into two tricopper oxo entities in CH_3NO_2 solution is confirmed by EPR results: **1** and **2** present each at room temperature a well-resolved four-line spectrum ($S = {}^1/_2$, $I = {}^3/_2$) with the Hamiltonian parameters $g_{iso} = 2.096$ and $A_{iso} = 87$ G. In each case, the signal integration was consistent with a doublet ground state $S = {}^1/_2$ per Cu^{II}_3 unit.

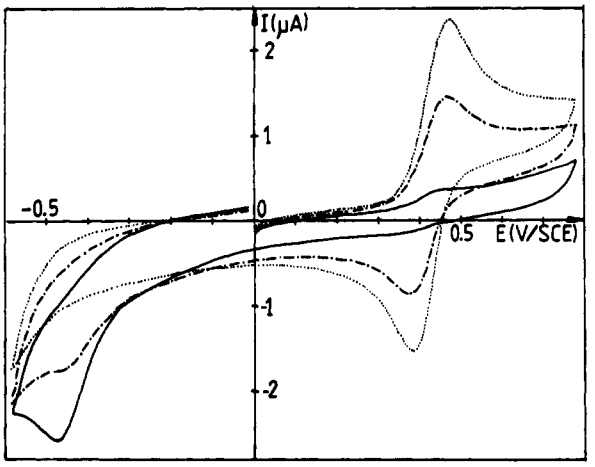

Figure 5. Effect of addition of triethylamine on **1** in PC + 0.1 M TBAP, Pt electrode, scan rate 100 mV s^{-1}: **1** ($c = 9.9 \times 10^{-4}$ M) (—); **1** + NEt_3 in 2/1 ratio (-·-); **1** + NEt_3 in 1/1 ratio (···).

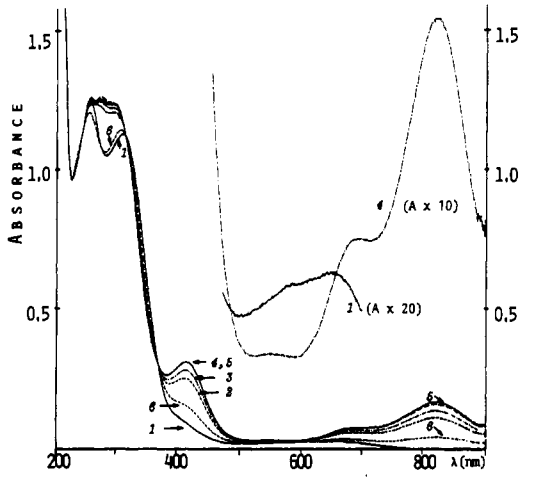

Figure 6. UV–vis spectral changes accompanying in situ spectroelectrochemistry of **2** in PC + 0.1 M TBAP: curves 1–5, oxidation of **2** at +0.70 V versus SCE; curve 6, oxidation followed by reduction at +0.20 V versus SCE.

SCE. Moreover, after being allowed to stand for a few days, the solution of **4** turns into **1** which was spectroscopically, electrochemically, and chemically (**1** ↔ **2** interconversion) characterized. This behavior is summarized on the right side of Scheme I.

Coulometric reduction of **1** shows that the reductions at −0.41 and −1.07 V versus SCE are respectively one- and two-electron exchanges. A metallic copper deposit is observed during coulometric reduction at −1.20 V versus SCE, indicating the breakup of the triangular Cu_3 core. This second irreversible step is observed for both **1** and **2**. The voltammetry on a solution of **1** reduced exhaustively at −0.70 V versus SCE containing **3** shows the remaining reduction step at −1.07 V versus SCE and a reversible monoelectronic oxidation step at +0.42 V versus SCE (Figure 3a) already observed in the cyclic voltammetry of **1** (Figure 4b). Coulometric oxidation at +0.70 V versus SCE of **3** involves one electron and shows the lack of the typical absorptions for the mixed-valence $Cu^{III}Cu^{II}$ compound and of the corresponding reduction at +0.42 V on RDE. *These features clearly confirm that it is a $Cu^{II}_2Cu^{I}$ compound that is oxidized at the same potential as* **2**. It may be assumed that **3** is a $[Cu^{I}Cu^{II}_2(OH)]^+$ species proceeding from a fast structural change which could be the chemical step in the EC reduction mechanism of **1**. **3** is now reversibly oxidizable on the time scale of cyclic voltammetry. The positive redox potential observed is indicative of a likely tetrahedral stereochemistry around the Cu(I) center. Moreover, after exposure to air, **1** is quite entirely regenerated from the solution of **1** initially reduced and further reoxidized. The proposed redox mechanism of **1** is given on the left side of Scheme I. The coincidence of identical values of redox potential for the couples $[Cu^{I}Cu^{II}_2(OH)]^+/[Cu^{II}_3(OH)]^{2+}$ and $[Cu^{II}_3(O)]^+/[Cu^{III}Cu^{II}_2(O)]^{2+}$ may be due to the fact that they are isoelectronic. To our knowledge such behavior has never been reported.

Scheme I

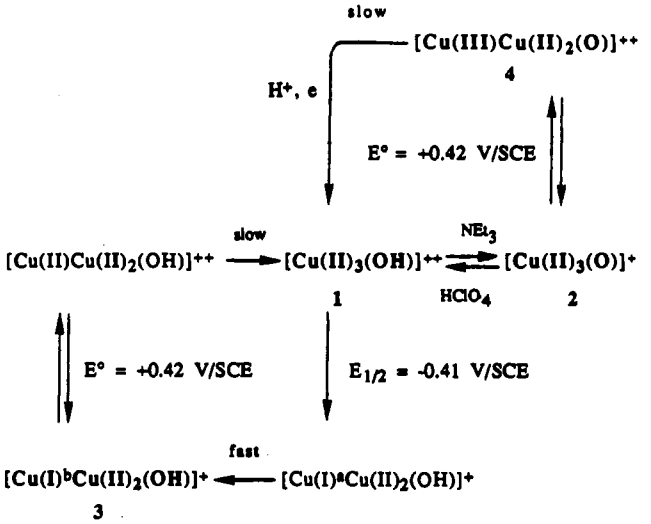

[a]Likely square-planar stereochemistry around Cu(I) ion. [b]Likely tetrahedral geometry around Cu(I) ion. Bold script corresponds to stable identified species.

1 and **2** provide an example of redox potentials driven by protonation, as occurs in many oxidase systems working in natural compounds,[40-43] the complex being oxidant or reductant depending on the protonation state of the Cu_3O core. Thus **1** and **2** play a chemical switch role between two redox reaction loops.

Acknowledgment. We thank Maxime Bernard for obtaining the EPR spectra and Dr. Jean-Jacques André for helpful discussions.

Supplementary Material Available: Tables of final thermal parameters, all bond lengths and angles, hydrogen atom coordinates, least-squares planes, and crystal data and collection parameters for **1** and **2** and a figure with the full contents of the asymmetric unit of **2** (22 pages); tables of calculated and observed structure factors for **1** and **2** (26 pages). Ordering information is given on any current masthead page.

(40) Mc Carty, R. E. In *Transport in Plants III*; Stocking, C. R., Heber, U., Eds.; Springer Verlag: New York, 1976; pp 347–376.
(41) Kok, B. In *Plant Biochemistry*, 3rd ed.; Bonner, J., Varner, J. E., Eds.; Academic Press: New York, 1976; pp 845–885.
(42) Mitchell, P. *Science* **1979**, *206*, 1148–1159.
(43) Malmström, B. G. *Chem. Rev.* **1990**, *90*, 1247–1260.